J. theor. Biol. (1994) **169**, 101–112

Design Principles of a Low Voltage Cardiac Defibrillator Based on the Effect of Feedback Resonant Drift

V. N. BIKTASHEV†‡ AND A. V. HOLDEN‡§

† *Institute of Mathematical Problems of Biology (formerly Research Computing Centre), Pushchino, Moscow Region,* 142292, *Russia and* ‡ *Department of Physiology and Centre for Nonlinear Studies, University of Leeds, Leeds LS*2 9*JT, U.K.*

(*Received on* 11 *March,* 1993, *Accepted in revised form on* 28 *February* 1994)

We explore the possibility of exploiting the phenomenon of the resonant drift of autowave vortices in the design of low-voltage cardiac defibrillators. The problem of reflection of resonantly drifting vortices by inexcitable boundaries is overcome by using feedback. Numerical studies show that the voltage needed for defibrillation by this method may be substantially less (by an order of magnitude) than that used in conventional single-shock defibrillation.

1. Introduction

Autowave vortices in heart tissue—spiral waves, reverberators, rotors, leading circles—are believed to underlie the dangerous cardiac arrhythmias of paroxysmal atrial tachycardia and ventricular fibrillation (Janse, 1991). It is important to be able to extinguish rapidly these pathological re-entrant waves. The current method of suppressing fibrillation in the heart, whatever its origin, is by applying a high-voltage stimulating pulse. The effectiveness of this method does not depend on the mechanisms responsible for the pathological re-entrant activity, as it forces the heart into a uniform resting state, out of which normal pacemaker-driven activity can emerge. However the current densities used can result in tissue damage. There is a real need for less damaging methods of cardiac defibrillation that, by exploiting specific features of re-entrant mechanisms, use low-voltage stimulation. Here we consider the possibility of exploiting the phenomenon of resonant drift in the design of a new type of defibrillator.

The phenomenon of resonant drift of autowave vortices was described by Davydov *et al.* (1988) and Agladze *et al.* (1987) and consists of directed motion of the autowave vortex if the autowave medium is driven by a spatially uniform periodic external forcing of appropriate frequency. It is widely believed that the mechanism of re-entrant cardiac arrhythmia and fibrillation are closely related to autowave vortices, and so it is natural to use resonant drift to drive vortices out of cardiac tissue and hence extinguish these dysrhythmias. In a previous paper (Biktashev & Holden, 1994) we presented numerical simulations that show repulsion of a resonantly drifting vortex from the inexcitable boundaries of the medium. This phenomenon makes the direct use of low-voltage resonant drift ineffective, and large external-forcing amplitudes (comparable to that of conventional single-pulse defibrillation) are required to overcome this repulsion.

The mechanism of this repulsion was explained in Biktashev & Holden (1994), using a simple phenomenological model based on the symmetry properties of the rotating vortex, and is summarized in Section 2.

This explanation makes it clear that any inhomogeneities in the autowave medium can have analogous effects. Therefore it should be expected that in reality a resonantly drifting vortex will not have a straight

§ Author to whom correspondence should be addressed.

trajectory at a given stimulating frequency, but will wander erratically, and when it approaches the vicinity of an inexcitable border it will be repelled.

However, the simple phenomenological model also suggests a way of overcoming both the effects of inhomogeneities and of reflection by boundaries. This is by changing the stimulating frequency as the frequency of the vortex changes, using feedback. In this paper we describe a simple phenomenological theory and some numerical experiments with a simple model of an autowave medium, and show that the use of feedback can substantially lower the threshold amplitude of the forcing that extinguishes the vortex by moving it to an inexcitable boundary. In our numerical experiments we have found that this threshold may be an order of magnitude lower than the single-shock defibrillation threshold. This provides a new principle for the design of a low-voltage defibrillator.

The structure of the paper is as follows. Section 2 is a short review of the phenomenon of resonant drift and of the problems related to its applications. In Section 3 we present the method of feedback stimulation. The relative effectiveness of different methods of stimulation for suppressing of vortices is assessed in Section 4. These results and their applicability to cardiac arrhythmias and dysrhythmias are discussed in Section 5.

Throughout the paper we present analytical considerations in parallel with illustrations for the phenomenological ODE system for resonant drift and numerical results for a simple PDE model of an excitable medium. Both ODE and PDE models are described in the Appendix.

2. Resonant Drift and the Resonant Repulsion

Autowave vortices may be considered mathematically as specific solutions to reaction–diffusion partial differential equations of the form

$$\partial u/\partial t = f(u) + D\nabla^2 u, \tag{1}$$

where u is a vector function (e.g. the vector of the transmembrane voltage and the activation and inactivation variables of the ionic channels of heart cells), f is a non-linear function (the ionic currents) and D is a diffusion matrix (of which only one component related to electric conductance is non-zero for cardiac tissue). These are solutions that have form of rotating spiral waves. In the simplest case of two spatial dimensions the vortex solutions have the form

$$u(x, y, t) = U(\rho(x - Y, y - Y), \theta(x - X, y - Y) - \omega t - \phi), \tag{2}$$

where ρ and θ are polar co-ordinates,

$$\rho(a, b)\cos(\theta(a, b)) = a; \quad \rho(a, b)\sin(\theta(a, b)) = b, \tag{3}$$

i.e. the vortex rotates rigidly with constant angular velocity ω. The co-ordinates X, Y of the rotation center and the phase ϕ of the rotation are arbitrary, due to symmetry of (2) with respect to shifts in space and time. A numerical solution of this sort for the PDE model given in the Appendix, in a bounded medium, is presented in Fig. 1.

Consider now the possible consequences of small perturbations of limited duration on the solutions of the form (2). Since we are interested primarily in applications to cardiac muscle, we will use the term "stimulation" instead of "perturbation". A characteristic feature of spiral waves in excitable media is their strong stability to perturbations, for topological reasons (Mikhailov, 1991); in fact a spiral wave can organize an entire excitable medium, annihilating other types of solution. So the vortex will not be destroyed or metamorphosed by the small amplitude stimulation but, after a time, will be restored. However, there is no reason for the arbitrary constants X, Y, ϕ to be restored to their previous values, i.e. the vortex will usually be shifted in space and time.

These spatial and temporal shifts will have an asymptotically linear dependence on stimulation amplitude for small stimulation amplitudes. Since the solution (2) is periodic in time, this dependence should be periodic in time.

Combining these two simple statements, we can conclude that a small-amplitude stimulation that is periodic in time, with a period equal to the period of rotation, should cause a directed drift of the vortex, with the direction of the drift being determined by the phase difference between the vortex rotation and the periodic stimulation. If the stimulation depends only on time but is uniform in space [e.g. it is caused by periodic change of parameters of the r.h.s. of (1)] then this drift will continue indefinitely and cause drift of the vortex for an arbitrarily large distance. Though we cannot predict *a priori* the drift direction and velocity caused by a particular stimulation, as it depends on the specifics of both the medium and the stimulation, we can state that a shift of the perturbation in time for, say, one half of the vortex rotation period will change the direction of the drift by 180°.

This statement is not strictly accurate since the phase of the rotation can also be changed by the stimulation. For it to be accurate we require that the

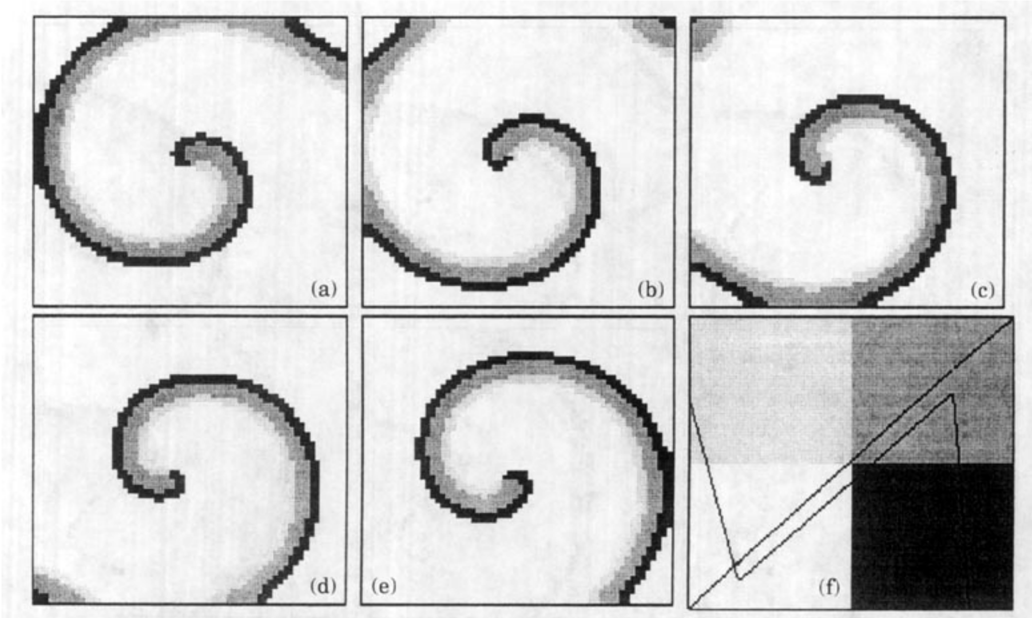

FIG. 1. The autowave vortex in the model medium (A.1–A.5). (a)–(e) Successive positions of the excited region in intervals is about one half of the medium size, the core size is of the order of one tenth of the medium size. (f) Phase plane of point system (A.1–A.4). The null-clines are shown. The shades the phase plane are used to display the states of points of the medium in (a)–(e); points not shaded at (a)–(e) are where $u < 0{\cdot}5$ and $v < 0{\cdot}5$.

frequency of stimulation is equal to "resonant" frequency that varies with the stimulation amplitude and tends to the frequency of unperturbed rotation as this amplitude tends to zero.

This leads to the idea of the resonant drift: if the whole medium is stimulated periodically in time and homogeneously in space, with a properly chosen period, then each stimulation pulse leads to the shift of the vortex to the same direction, and as a result, the average vortex position drifts along a straight line.

The dependence of the resonant period and the velocity of resonant drift on the stimulation amplitude for our PDE model are shown in Fig. 2, and the idea of the resonant drift is illustrated on Fig. 3. We can see from Fig. 2 that for small enough amplitudes both dependencies are linear.

Resonant drift was first predicted for an analytical model [not a reaction-diffusion system like (1)] for an autowave medium with very specific properties (Davydov *et al.*, 1988) and was then experimentally observed in Belousov–Zhabotinsky reaction medium (Agladze *et al.*, 1987). The above considerations show that resonant drift is not restricted to a few specific media—even the form (1) is not necessary—but is determined only by symmetry and stability properties, and so is to be expected in all models for cardiac tissue that have vortices with these symmetry and stability properties.

Our phenomenological theory for resonant drift of a single vortex proposed in Biktashev & Holden (1994) considers the motion of the vortex core to be governed by the ODE system:

$$\mathrm{d}x/\mathrm{d}t = v(x, y)\cos\varphi + C_x(x, y) \tag{4}$$

$$\mathrm{d}y/\mathrm{d}t = v(x, y)\sin\varphi + C_y(x, y), \tag{5}$$

where x and y are co-ordinates of the core [denoted X, Y in (2)], φ is the phase difference between the stimulation and vortex rotation [the latter was denoted ϕ in (2)], v is the resonant drift velocity, and

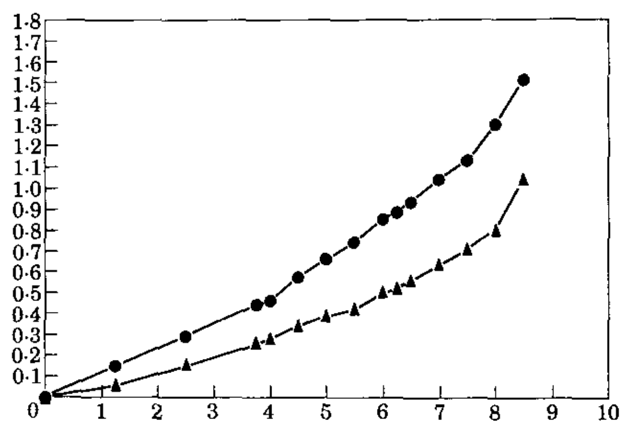

FIG. 2. The parameters of resonant drift at various forcing amplitudes. They were chosen to achieve a straight drift parallel to the y-axis far from boundaries at some initial phase. The boundary conditions at upper and lower boundaries are periodic. Abscissa: stimulation amplitude $A \times 100$; (●): (reciprocal resonant frequency minus that for free vortex) × 100 (time steps)$^{-1}$; (▲): resonant drift velocity × 100 space steps (time step)$^{-1}$. The single pulse defibrillation threshold, which physically corresponds to a large stimulus, is about 0·2, i.e. 20 in this scale.

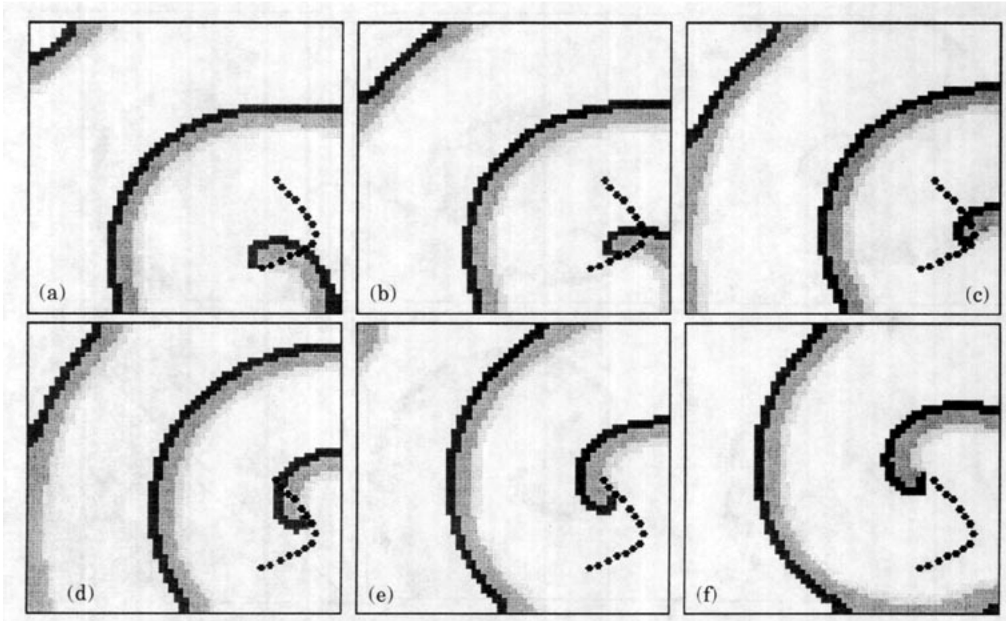

FIG. 3. Illustration to the mechanism of resonant repulsion. Stimulation amplitude $A = 0{\cdot}055$ homogeneous over the medium, period 251 time steps. Here and below, the boundaries are impermeable. (a)–(f) Successive positions of vortex in time intervals of exactly three periods of stimulation. The trajectory of the core is shown by black dots at each picture.

C_x, C_y describe drift of the vortex caused by other reasons, such as inhomogeneity of the medium, interaction with other vortices or with boundaries. If the stimulation has a constant frequency, then the equation for the phase difference can be written

$$\mathrm{d}\varphi/\mathrm{d}t = \omega(x, y) = \Omega_r(x, y) - \Omega_s, \tag{6}$$

where Ω_s is the stimulation frequency and Ω_r is the vortex rotation frequency, which in general depends on its position in the medium because of the effects of inhomogeneity or interactions. It is easy to see that with $C_x = C_y = 0$ and constant v, $\omega \neq 0$ the trajectories are circles, while at $\omega = 0$ they are straight lines.

The problem is to find conditions so that the trajectory of the core will reach the boundaries of the medium, for this is the only way to extinguish a single vortex gently. The naive idea is that since it is possible to cause the vortex to drift in a certain direction it will always reach a boundary. The reality is more complicated. First, since Ω_r is a function of the spatial co-ordinates there can be no exact resonance for the whole medium. The trajectory will not be straight but have some complicated form, and we can only hope that it will ultimately reach a boundary. Second, there is the repulsion effect caused by the regular change of rotation frequency in the vicinity of a boundary, described in Biktashev & Holden (1994). Owing to this effect, even if the trajectory approaches the boundary, it will be reflected and the vortex survives—this behaviour was described in Biktashev & Holden (1994).

Figure 3 illustrates the mechanisms of this effect. When the core is far from the boundary, the resonance is sufficiently exact and each new stimulus occurs at the same rotation phase, therefore each subsequent shift is in the same direction. The closer the vortex is to the boundary the faster is its own rotation and the stimuli occur at later and later phases, thus changing the direction of shifts, and the trajectory curves. This process continues until the vortex is again far from the boundary.

Figure 4 shows some typical trajectories of the vortex core during resonant drift for the PDE model and the phenomenological ODE system; it can be seen that at this stimulation amplitude the vortex never touches the boundary and persists a very long time after stimulation.

This simple explanation does not take into account the role of the terms C_x, C_y in (4) and (5). The analysis made in Biktashev & Holden (1994) shows that in the presence of these terms repulsion of the vortex by the boundary also takes place. This repulsion may be overcome only if there is an attraction of the vortex to the boundary owing to the terms C_x and C_y, but even in this case this would probably lead to attaching the vortex to the boundary rather than its annihilation. We have not seen, and are not aware of any examples in the literature, of the spontaneous disappearance of vortices owing to their attraction to boundary, except in the case of very small areas of an excitable medium.

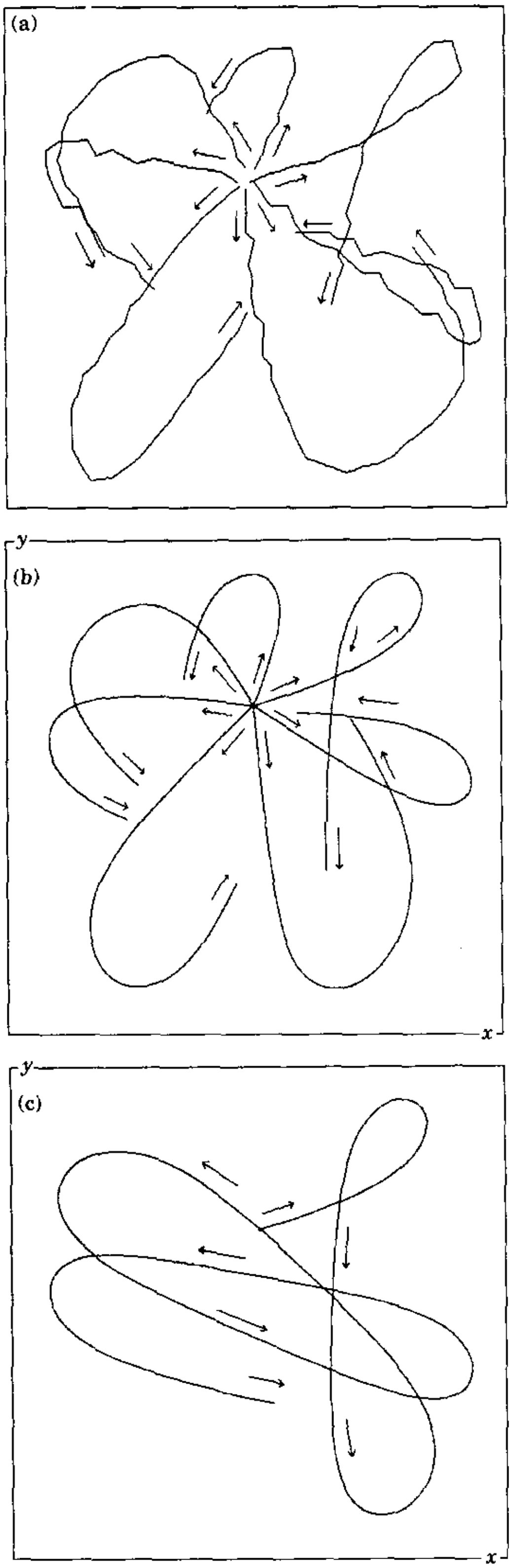

Fig. 4

FIG. 4. Resonant drift produced by constant frequency stimulation. (a) Trajectories of the vortex core in PDE model with various initial phase of external forcing. Period of stimulation is 254 time steps, $A = 0{\cdot}050$, the initial phases are chosen equidistant with interval of 40 time steps. All the trajectories show repulsion from boundaries at these parameters. (b) Trajectories of ODE model (4–7) (A.11–A.16) with $v = 0{\cdot}007$, the initial phases chosen equidistant with interval $2\pi/7$. Compare with (a). (c) A long piece (time interval 45 000) of one of the trajectories shown in (b).

3. Resonant Drift Driven by Feedback

A way to overcome both the problems of the unknown resonant frequency and the resonant repulsion from the boundary is to change the frequency or phase of stimulation as the vortex rotation frequency or phase changes. This can be achieved using feedback. For the case of feedback we can describe the phase difference φ in (4) and (5) not by an ODE such as (6) but by a fixed dependence on the current position of the vortex:

$$\varphi(t) = \Phi(x(t), y(t), x_r, y_r). \qquad (7)$$

One of the simplest ways to produce such a feedback is to apply stimuli at the times the excitation wavefront reaches a particular recording point in the medium, or after a certain delay after this recording; the position of the recording point is denoted x_r, y_r in (7).

This can be realized by a simple device that consists of (i) a recording electrode, which measures the voltage at a point in the tissue, and a trigger that monitors the arrival of the excitation wave at this point; (ii) a timer, which controls a delay time (that may be zero) between the arrival of the excitation wave and stimulation via a stimulating electrode; (iii) that influences the whole tissue, possibly homogeneously, by an electric pulse of a specified amplitude and duration. Naturally, the recording electrode should not be active during the stimulation pulse.

In this case the function Φ in (7) will be equal to the phase distance from the core to recording point plus the delay between the stimulus and the vortex rotation frequency plus some unknown constant that varies with the properties of the medium. Assuming that the shape of the vortex is described by an Archimedean spiral, we may write

$$\Phi(x, y, x_r, y_r) = \theta(x - x_r, y - y_r) + 2\pi\rho(x - x_r, y - y_r)/\lambda + \delta, \qquad (8)$$

where ρ, θ are defined by (3), λ is the asymptotic wavelength and the symbol δ denotes the sum of the stimulation delay and the unknown constant determining the direction of the resonant drift at a particular stimulation phase.

Typical trajectories of systems (4), (5), (7) and (8) at $C_x = C_y = 0$ are shown in Fig. 5. It can be seen that

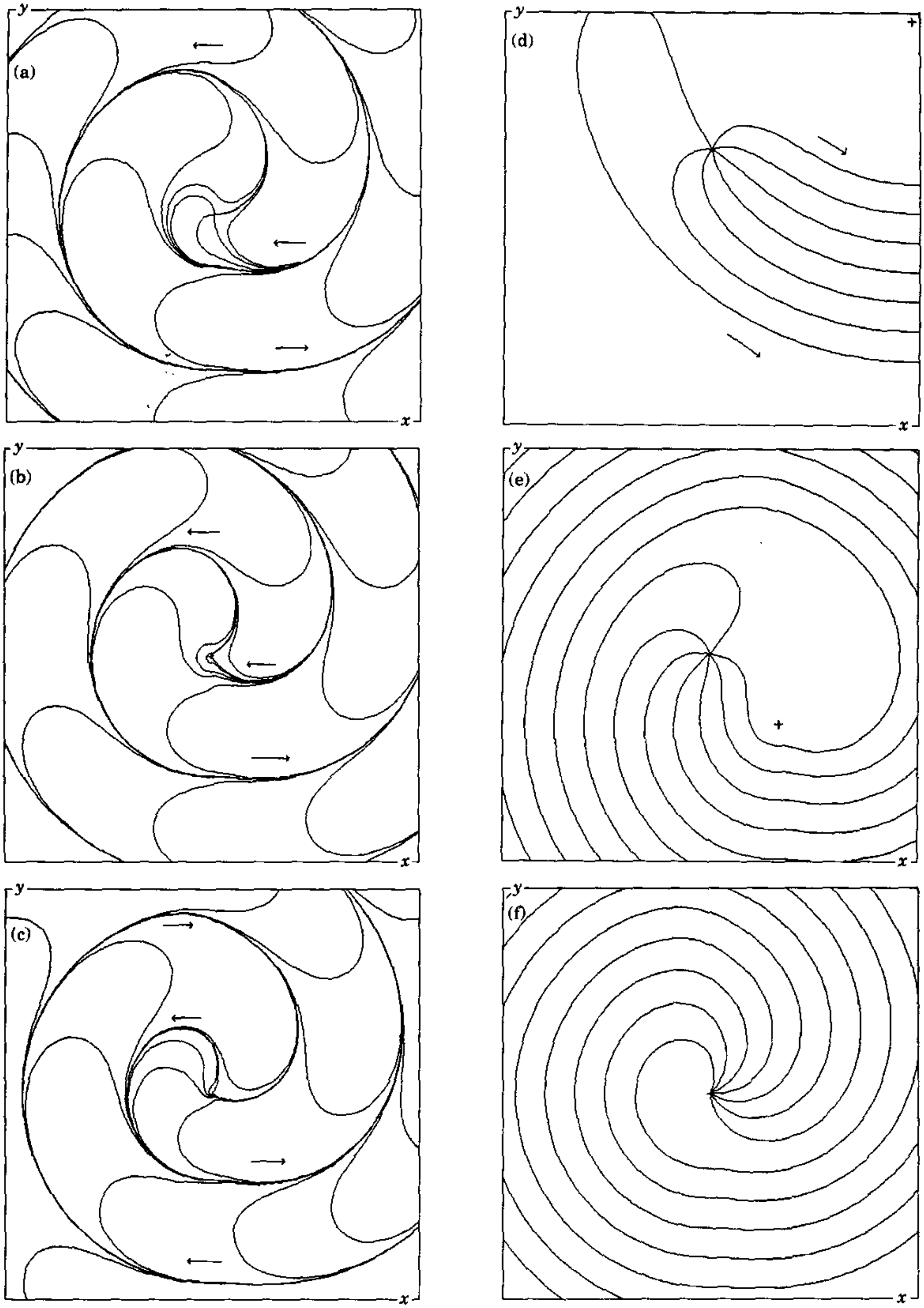

FIG. 5. The feedback RD trajectories for the system (4), (5), (8), (A.11), (A.16) at $C_x = C_y = 0$. (a)–(c) The phase portraits of the system at δ equal to 0, $\pi/3$ and $2\pi/3$, respectively. Note that at $\delta = \pi$, $4\pi/3$ and $5\pi/3$ the portraits are the same with reversed directions of trajectories. The position of the recording electrode (in centre) is seen as the singular point at the portraits. (d)–(f) The bundles of trajectories emerging from the same initial point at different phase delays (0, $\pi/3$, $2\pi/3$, etc), shown for three different initial points and recording points. The recording point is shown by a cross in each panel, in (f) it coincides with the initial point.

the recording point is always a singular point in phase portraits, but its particular type is not of interest since the approximation (8) obviously is not valid as (x, y) is close to (x_r, y_r). It is only important to note that all the trajectories are not closed and leave any finite region independent of the specific value of the constant δ.

It is reasonable to expect that taking account of the terms C_x, C_y in (4) and (5) would make the behaviour of trajectories more complicated. In particular, if their typical value is large compared to the resonant drift velocity v and their sign corresponds to repulsion form the boundary, then the trajectories will not reach the boundary. This is confirmed by simulation: in Fig. 6 it can be seen that for large values of v all trajectories reach the boundaries, for smaller values of v all do not.

4. On the Effectiveness of Various Methods of Defibrillation

We see that even in the case of feedback stimulation, there are threshold values for the stimulation amplitude [which in phenomenological systems (4) and (5) are represented by the parameter v] that are necessary and sufficient for extinguishing the vortex by resonant drift to a boundary. There is also a threshold for stimulation amplitude below which extinguishing the vortex is impossible in the case of resonant drift produced by constant frequency stimulation. We now compare these thresholds; we use for these estimations the same exponential form for interaction with boundary that was used in Biktashev & Holden (1994):

$$\omega(x, y) = a \exp(-x/R) \tag{9}$$

$$C_x = b \exp(-x/R) \tag{10}$$

$$C_y = c \exp(-x/R). \tag{11}$$

Here we assume that the medium is located at $x \geqslant 0$; R is the characteristic length of the interaction with the boundary, and a, b, c are constants, $a > 0$, $b > 0$ (this is a generalization of the interaction dependencies that were obtained for a specific autowave medium in Biktashev, 1989).

For the case of constant frequency stimulation i.e. for trajectories of systems (4–6), we find the leftmost position of the core at all possible time moments and initial phases,

$$x_{cf} = \min\{x(t) | x(-\infty) = +\infty,$$
$$\varphi(-\infty) \in (\pi/2, 3\pi/2), \quad t \in (-\infty, +\infty)\}. \tag{12}$$

Using the parametric form for the solutions (4–6), (9–11) obtained in Biktashev & Holden (1994)

$$x = -R \log(a^{-1} \mathrm{d}\varphi/\mathrm{d}t) \tag{13}$$

$$\mathrm{d}\varphi/\mathrm{d}t = -vR^{-1} \sin(\varphi + \theta)\cos(\theta) + C \exp(-v\varphi) \tag{14}$$

$$v = \tan(\theta) = b/(aR); \quad \theta \in (-\pi/2, \pi/2), \tag{15}$$

the minimum (12) can be written as

$$x_{cf} = -R \log(v(aR)^{-1}(1 + v^2)^{-1/2} E(v)), \tag{16}$$

where the function $E(\,)$ has a simple geometrical interpretation (see Fig. 7). Note that this function is both bounded

$$1 < E(v) < 2, \quad v \in (0, +\infty), \quad E(0) = 2,$$
$$E(+\infty) = 1, \tag{17}$$

and monotonically decreasing, so x_{cf} in (16) grows monotonically with b. The condition that the minimal value of x should lie beyond the boundary, which is a necessary condition for annihilation, is therefore

$$v > v_{cf} = aR(1 + v^2)^{1/2} E(v)^{-1}. \tag{18}$$

We assumed that the critical position for the vortex is $x = 0$; choosing any other position does not influence the comparison.

For the case with feedback, the necessary condition for the existence of trajectories that cross the line $x = 0$ from right to left is simply

$$v > v_{fb} = b. \tag{19}$$

Comparison of (18) and (19) shows that

$$v_{fb}/v_{cf} = v(1 + v^2)^{-1/2} E(v) < 1; \quad v = b/(aR), \tag{20}$$

i.e. that feedback stimulation always needs smaller (and for the case $b/(aR) \ll 1$ very much smaller) amplitudes for extinguishing a vortex by resonant drift than constant frequency stimulation.

The simple reason for the validity of inequality (20) is that in the case of feedback stimulation only the effect of spatial interaction with the boundary (characterized by the coefficient b) should be overcome, while at constant frequency both spatial and temporal (characterized by a) effects are dealt with, and it is natural that the relative effectiveness of these stimulations depends on the dimensionless ratio $b/(aR)$.

The probabilities of vortex elimination in the PDE model by different "defibrillation techniques" are presented in Fig. 8, including classical single-pulse defibrillation, and defibrillation by resonant drift to a boundary for constant-frequency, stimulation and feedback stimulation. The probability is obtained

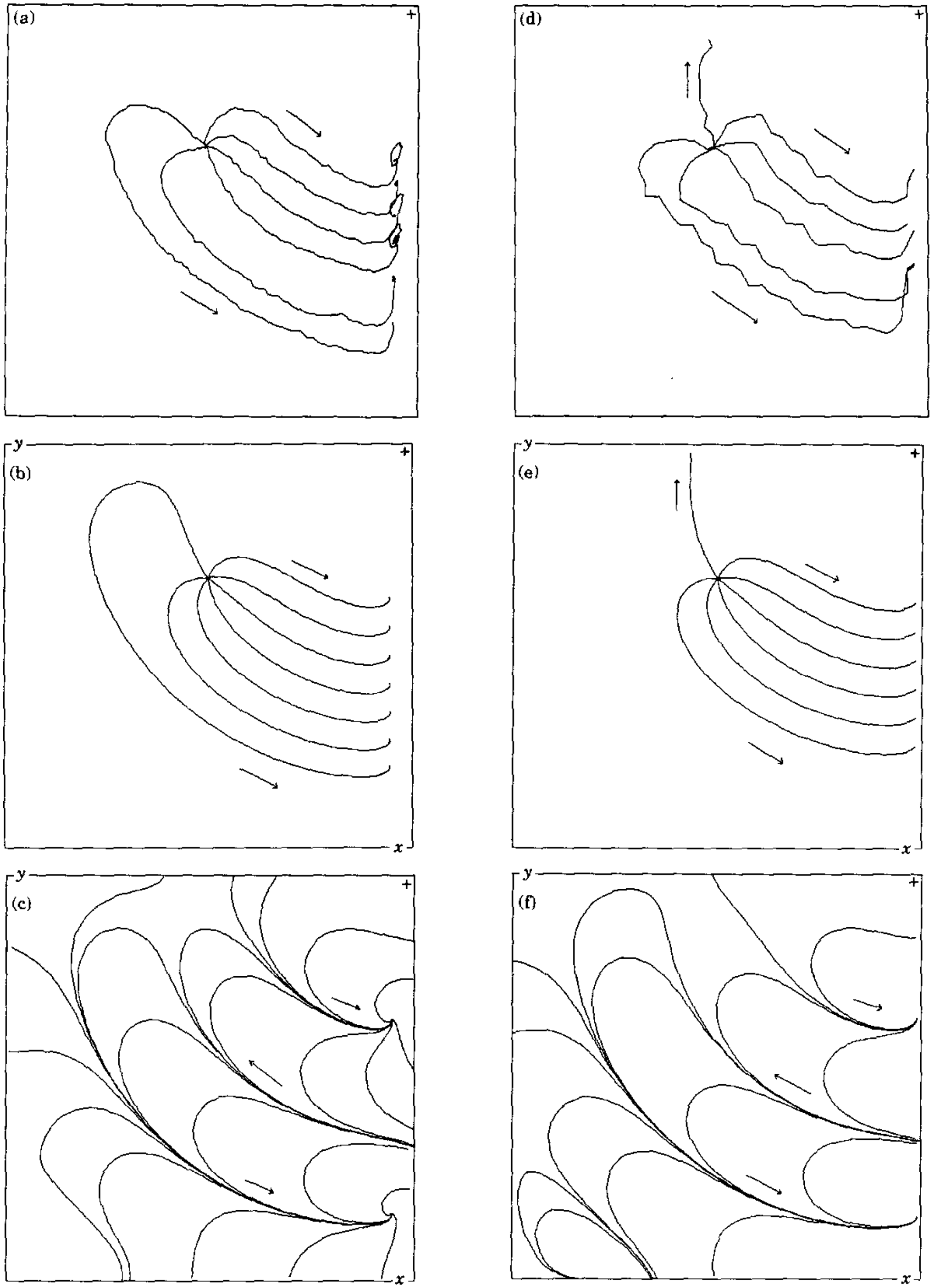

FIG. 6. The feedback resonant drift trajectories for the systems (4), (5), (8), (A.11–A.16) at non-zero C_x, C_y ($b = 0{\cdot}005$, $c = 0{\cdot}003$) and the trajectories of core in PDE simulation. (a) PDE trajectories, $A = 0{\cdot}025$, delays from 0–200 time steps equidistant with 40 time steps. The vortex does not annihilate at either delay. (b) ODE trajectories, $v = 0{\cdot}0025$, δ equidistant in $2\pi/7$. (c) Phase portrait of ODE system at $v = 0{\cdot}0025$ and $\delta = 0$. (d) Same as (a), $A = 0{\cdot}050$. The vortex annihilates for each delay. (e) Same as (b), $v = 0{\cdot}005$. The trajectory computation was stopped if it reached less than 1 space step from a boundary; this occurred for all trajectories. (f) Phase portrait of ODE system at $v = 0{\cdot}005$ and $\delta = 0$.

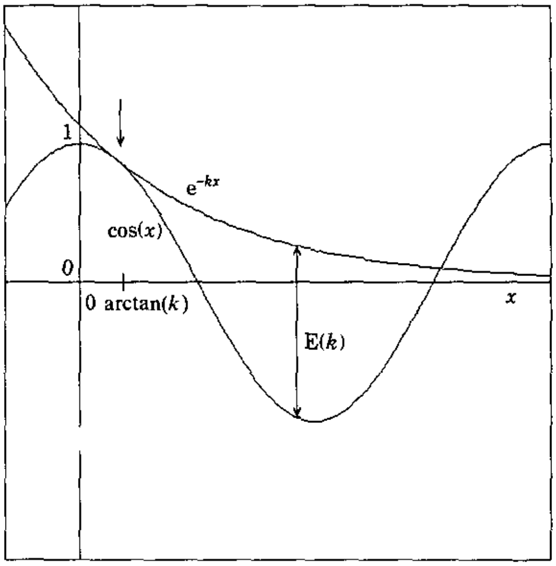

FIG. 7. The geometrical definition for the function $E(k)$ in (16). The graphs of the functions $\cos(x)$ and $C\,e^{-kx}$ are drawn, with constant C chosen so that the curves are tangent at $x = \arctan(k)$ (shown by arrow). The function $E(k)$ for this value of k is the maximal distance between this curves to the right of the touching point (shown by arrows). It can be seen that $1 < E < 2$ and E diminishes with k.

from taking an average over a number of experiments (from ten to 30) over a randomly chosen phase, where phase is relative to the phase of the vortex, and is obtained from the occurrence time for a single defibrillating pulse, the initial time for beginning of periodic series of stimulation, and the delay time for feedback stimulation. In the last case the delay should not be more than the period of rotation minus the length of the stimulus. For the constant-frequency curve the period of stimulation was chosen as close to resonance as possible (within the constraints of the discrete time lattice) from the values given in Fig. 2.

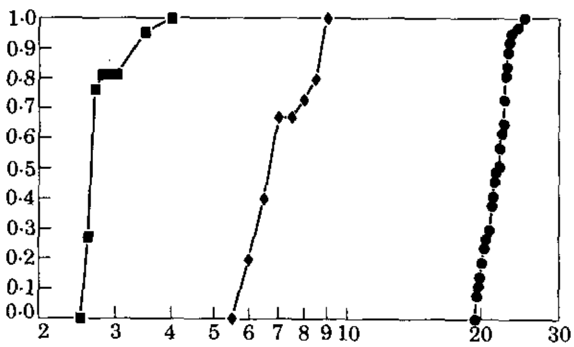

FIG. 8. Comparison of effectiveness of different methods of stimulation. Abscissa: the stimulation amplitude × 100. Ordinate: the probability of annihilation of the vortex with occasionally chosen phase parameter. Initial position of vortex for all experiments is close to a center of the medium. (●): single-pulse stimulation (classical defibrillation); (◆): constant frequency stimulation, with resonant frequency; (■): feedback stimulation.

In fact this curve (b) is only theoretical, as it is impossible in practice to obtain an exact resonant frequency, as the resonant frequency varies with different positions of the vortex in the medium.

5. Discussion

We have shown for both the two-dimensional PDE model and the phenomenological ODE model that the reflection of a resonantly drifting vortex by a boundary can be overcome by using feedback-controlled stimulation, and that the threshold for extinguishing a resonantly drifting vortex using feedback is less than the thresholds using a single defibrillating shock. In the example considered the threshold is an order of magnitude less. The method is based on the symmetry of a rigidly rotating vortex, and so resonant drift, the reflection of a resonantly drifting vortex by a boundary, and overcoming this by feedback, will apply for all vortices with these properties. Such vortices are generated by biophysically derived excitation equations, such as the Noble (1962) model with standard parameter values and the Beeler–Reuter (Beeler & Reuter, 1977) equations (Courtemanche & Winfree, 1991; Panfilov & Holden, 1991) and presumably are generated for reasonable parameter sets by the Oxsoft (1988) models for atrial and ventricular muscle. Thus this method should be effective for vortices in these models.

However, vortices in real cardiac tissue are asymmetric, owing mainly to anisotropy in conduction pathways, are three dimensional rather than two dimensional, and (especially in the ventricle) are multiple, as vortex breakdown kindles new vortices.

Although the method has only been illustrated for symmetric vortices, we expect it to be robust for asymmetric vortices associated with linear, elliptical and Y-shaped cores or areas of functional conduction block (Dillon *et al.*, 1985; Panfilov & Holden, 1993). Although such vortices may be obtained numerically in an isotropic, homogeneous excitable medium (Krinsky *et al.*, 1992) the mechanism of asymmetric vortices in cardiac tissue is not clear and so the effectiveness of the method for asymmetric vortices requires further numerical investigations with asymmetric vortices produced in both isotropic and anisotropic models. The effectiveness of the method for asymmetric vortices in cardiac tissue is probably best evaluated by acute animal experiments, rather than by numerical investigations.

Another problem may arise owing to strong inhomogeneities in cardiac tissue, which can cause strong C_x, C_y fields interfering with the RD. For instance, inhomogeneities may lead to "pinning" of the vortex to a local defect in the medium (Vinson *et al.*, 1994), and this effect can influence the resonant drift trajectory. We anticipate that this influence will be analogous to that of the C_x, C_y fields near the boundaries, and so can be overcome by stimulation of an appropriate amplitude. Further investigation of interaction between RD and various types of medium inhomogeneities is needed.

Preliminary experiments with the PDE model in three dimensions have shown that resonant drift with feedback is effective in extinguishing vortices in an isotropic, homogeneous medium with absorbing boundaries. However, given the richness of vortex behaviour in three dimensions with vortex filament twist, tension, and drift, the effects of boundaries and resonant drift in three-dimensional media requires further exploration.

In the case of multiple vortices (fibrillation), the approach also promises positive results. Since colliding wavefronts annihilate, the recording electrode will monitor the activity of only one vortex at a time. The course of events may be as follows. First, the vortex that influences the recording electrode is driven by resonant drift under feedback, which causes the directed drift of at least one vortex. On reaching the boundary, this vortex is extinguished and the electrode monitors the wavefront from another vortex, wich in turn is extinguished. If the vortices are extinguished more frequently than they are born, the method will eliminate all the multiple vortices.

Of practical importance is the time needed for extinguishing vortices by the proposed feedback resonant drift technique. It can be simply estimated from the path taken by the vortex, which is of the order of the medium size, divided by the RD velocity which is dependent on the stimulation amplitude (see Fig. 2). In our numerical experiments, at stimulation amplitude 0·03 (about 12% of the defibrillation threshold, annihilation probability 80%), a typical RD trajectory until annihilation was about 50 vortex rotations, which in ventricular tissue would correspond to a few seconds, if we scale time by the vortex period. However, as the resonant drift velocity is strongly dependent on the medium properties, realistic estimations of this time require simulations using biophysically derived models and *in vitro* experiments.

We are thankful to Professors E. E. Shnol, V. I. Krinsky and A. T. Winfree and Drs A. M. Pertsov and A. V. Panfilov for useful discussions and critical comments.

This work was partially supported by NATO grant CRG 920656, Wellcome Trust grant 03881712 (Leeds) and by the Russian Fund for Fundamental Research grant 93-011-068 (Pushchino).

REFERENCES

Agladze, K. I., Davydov, V. A. & Mikhailov, A. S. (1987). An observation of resonance of spiral waves in distributed excitable medium. *Pis' ma v ZETP* **45**, 601–603 (in Russian, English translation in *Sov. Phys. JETP Lett.*).

Beeler, G. W. & Reuter, H. J. (1977). Reconstruction of the action potential of ventricular myocardium fibers. *J. Physiol.* **268**, 177.

Biktashev, V. N. (1989). Drift of a reverberator in an active medium due to interaction with boundaries. In: *Nonlinear Waves II. Dynamics and Evolution* (Gapanov-Grekhov, A. V., Rabinovich, M. I. & Engelbrecht, E. J., eds). Berlin: Springer-Verlag.

Biktashev, V. N. & Holden, A. V. (1993). Resonant drift of the autowave vortex in a bounded medium. *Phys. Lett. A*, **181**, 216–224.

Courtemanche, M. & Winfree, A. T. (1991). Re-entrant rotating waves in a Beeler–Reuter based model of two dimensional cardiac electrical activity. *Int. J. Bifurcation & Chaos* **1**, 431–444.

Davydov, V. A., Zykov, V. S., Mikhailov, A. S. & Brazhnik, P. K. (1988). Drift and resonance of spiral waves in distributed media. *Izv. Vuzov Radiofizika* **31**, 574–582 (in Russian, English translation in *Sov. Phys. Radiophys*).

Dillon, S., Ursell, P. S. & Wit, A. L. (1985). Pseudo-block caused by anisotropic condition: a new mechanism for sustained re-entry, *Circulation* **72**(Suppl. III), 1116.

Janse, M. J. (1991). Re-entrant arrhythmias. In: *Heart and Cardiovascular System*, 2nd edn (Fozzard, H. A. *et al.*, eds) New York: Raven Press.

Krinsky, V. I., Efimov, I. R. & Jalife, J. (1992). Vortices with linear cores in excitable media. *Proc. R. Soc. Lond.* **A437**, 645–655.

Levitin, V. (1990). *TraX—Simulation and Analysis of Dynamical Systems.* Exeter Software. Setauket, New York.

Mikhailov, A. S. (1991). Kinematics of wave patterns in excitable media. In: *Nonlinear Wave Processes in Excitable Media* (Holden, A. V., Markus, M. & Othmer, H. G., eds) pp. 127–144. New York: Plenum.

Noble, D. (1962). A modification of the Hodgkin–Huxley equations applicable to Purkinje fibre action potentials and pacemaker potentials. *J. Physiol* **160**, 317–352.

Oxsoft (1988). *HEART Program Manual, Version 2.1.* Oxford: Oxsoft.

Panfilov, A. V. & Holden, A. V. (1991). Spatiotemporal irregularity in a two-dimensional model of cardiac tissue. *Int. J. Bifurcation Chaos* **1**, 219–225.

Panfilov, A. V. & Holden, A. V. (1993). Computer simulation of re-entry sources in myocardium in two and three dimensions. *J. theor. Biol.* **161**, 271–285.

Panfilov, A. V. & Pertsov, A. M. (1984). Vortex ring in a three-dimensional active medium described by a reaction–diffusion system. *Doklady Akademii Nauk* **274**, 1500–1503 (in Russian).

Rudenko, A. N. & Panfilov, A. V. (1983). Drift and interaction of vortices in a two-dimensional inhomogeneous active medium. *Studia Biophysica* **98**, 183–188.

Vinson, M., Pertsov, A. M. & Jalife, J. (1994). Anchoring of vortex filaments in 3D excitable media. *Physica D*, in press.

Winfree, A. T. (1991). Varieties of spiral wave behaviour. *Chaos* **1**, 303–34.

APPENDIX

The Numerical Models

Though for clinical purposes it would be more appropriate to investigate properties of feedback resonant drift for some biophysically derived models, such as the Oxsoft package of equations (Oxsoft,

1988) this is computationally expensive. Further, these models are still under development and as ODEs yield quantitative agreement to experimental results only for "point", not spatially distributed systems. Here we have restricted ourselves to the simplest (in a computational sense) qualitative model of an autowave medium. This approach is justified since the resonant drift effect is based on the symmetry properties of a rigidly rotating vortex, and so is a general phenomenon.

The numerical model derives from the Panfilov–Pertsov model (Panfilov & Pertsov, 1984) widely used by many authors (see, e.g. Rudenko & Panfilov, 1983; Winfree, 1991), and is a piecewise linear ODE of the form

$$\begin{cases} u_t = f(u) - v + \nabla^2 u + F(t) \\ v_t = \epsilon(u)(gu - v), \end{cases} \quad \text{(A.1)}$$

where $f(u)$ is an N-shaped piecewise linear continuous function

$$f(u) = \begin{cases} -g_1 u, & u < u_1 \\ -g_1 u_1 + g_f(u - u_1) & u_1 < u < u_2 \\ g_2(1 - u) & u > u_2, \end{cases} \quad \text{(A.2)}$$

$\epsilon(u)$ is a piecewise constant function,

$$\epsilon(u) = \begin{cases} \epsilon_1, u < u_1 \\ \epsilon_2, u_1 < u < u_2 \\ \epsilon_3, u > u_2. \end{cases} \quad \text{(A.3)}$$

and the parameter values are:

$$g = 1{\cdot}0, \quad g_1 = 4{\cdot}0, \quad g_f = 0{\cdot}98, \quad g_2 = 15,$$
$$u_1 = 0{\cdot}08, \quad \epsilon_1 = 1{\cdot}68, \quad \epsilon_2 = 0{\cdot}06, \quad \epsilon_3 = 1{\cdot}50. \quad \text{(A.4)}$$

Calculations were performed by the explicit Euler method with five-node approximation of the Laplacian on a rectangular grid of 60 × 60 internal nodes with the time step equal to 0·08 and space step equal to 0·8, with impermeable boundaries

$$\left.\frac{\partial u}{\partial x}\right|_{x = x_{min}, x_{max}} = \left.\frac{\partial u}{\partial y}\right|_{y = y_{min}, y_{max}} = 0, \quad \text{(A.5)}$$

or with periodic boundary conditions for $y = y_{min}, y_{max}$ (for Fig. 2).

The external stimulation was simulated as a time-dependent additive term $F(t)$ in the r.h.s. of the equation for u in (A.1) which corresponds to an external electric current applied to cardiac tissue. The time dependence of $F(t)$ was of the form of a series of rectangular pulses of duration of 50 time steps, with amplitude A varying in different experiments. For investigation of constant-frequency stimulation, the interval between stimuli as well as the initial time were varied. For the case of feedback stimulation, the free parameters were the position of the recording electrode and the delay of beginning of stimulus after recording the excitation wavefront at this electrode. The beginning of the excitation wavefront was determined simply by the time when the value of u at that point crossed a threshold, which was chosen as 0·5 in our experiments.

To determine the position of the vortex, the following procedure was used. At first, the maximum of u over one vortex period was calculated at every grid point:

$$u_m(x, y, t) = \max\{u(x, y, \tau), \quad \tau \in (t - \Delta t/2, t + \Delta t/2)\}, \quad \text{(A.6)}$$

for the time moments $t = n\Delta t$, $n = 1, 2, \ldots$ These are equidistant with a period Δt, chosen to be 280 time steps, which is a little longer than the period of the vortex (which was within the range 200–280 time steps in different situations). Next, the amount u_m was below some threshold value u_{th}, chosen to be 0·8 or 0·85 in our experiments, was calculated:

$$u_d(x, y, t) = \begin{cases} u_{th} - u_m(x, y, t), & \text{if } u_m(x, y, t) < u_{th}, \\ 0, & \text{otherwise} \end{cases} \quad \text{(A.7)}$$

Finally, the "center of mass" of the function u_d at the moment t was calculated

$$x_c(t) = \int u_d(x, y, t) x \, dx \, dy / M(t), \quad (A.8)$$

$$y_c(t) = \int u_d(x, y, t) x \, dx \, dy / M(t), \quad (A.9)$$

where

$$M(t) = \int u_d(x, y, t) \, dx \, dy. \quad \text{(A.10)}$$

The co-ordinates x_c and y_c were found to be quite convenient approximations for the rotation centre of the vortex. They do not require much time for calculation and have the advantage that their value may not lie on the nodes of the grid. This fact is especially important if we recall that the grid spacing is rather coarse.

The direct numerical experiments with the PDE model (A.1–A.5) were accompanied by simulations of the phenomenological ODE system (4–6) for continuous frequency stimulation and (4), (5), (7), (8) for feedback stimulation, with

$$v(x, y) = v = \text{const}, \tag{A.11}$$

$$C_x(x, y) = b(G(x) - G(L - x)) \tag{A.12}$$

$$C_y(x, y) = b(G(y) - G(L - y)) \tag{A.13}$$

$$\omega(x, y) = a(G(x) + G(L - x) + G(y) + G(L - y)) \tag{A.14}$$

$$G(x) = \mathrm{e}^{-x/R} \tag{A.15}$$

$$R = 4{\cdot}0, \quad a = 0{\cdot}005, \quad b = 0{\cdot}005, \quad L = 60, \quad \lambda = 30, \tag{A.16}$$

and v, δ, $x(0)$, $y(0)$ $\varphi(0)$ as free parameters (differing for different experiments). The parameter values (A.16) were chosen to achieve qualitative and possibly quantitative correspondence, in terms of space and time steps, with the PDE solutions. The phenomenological system was investigated using the program TraX (Levitin, 1990).